likely to interfere with the range of sterically allowed ϕ_{CN}, the CD spectra of the corresponding nucleosides are very similar.

The calculations using the couple oscillators described above are straightforward; we found that only a very narrow range of effective moment direction is available that satisfies the requirement of giving the correct sign for the CD of the two transitions. The optimum results for the two transitions were normalized separately for comparison with the experimental rotatory strengths; these coincide with the correlation curves in Figure 6 for the long-axis transition but deviate somewhat from those for the short-axis transition as shown by the dashed lines in Figure 6. The induced moments used in these calculations for both sets of anomers point approximately from the C_1' to the C_2' atom forming an angle with the $O_1'C_1'C_2'$ plane as shown in Figure 7 where the C_1'–C_2' bond is drawn in the plane of the page. It is seen that the induced moments are at an approximately mirror-image relationship with respect to the base in the two sets of anomers; this would agree with the different sugar puckering known to be endo for the β anomers[53] and exo for the α anomers.[68] The additional difference in sugar backbone conformations due to the position of the C_5' atom may explain why the angles between the induced moment directions, $\mathbf{e}_\alpha$ and $\mathbf{e}_\beta$, and the C_1'-C_2' bond differ in the two sets of anomers.

The results demonstrate the usefulness of the simple coupled oscillator model: trends and signs of the CD of transitions in adenine as a function of ϕ_{CN} are reproduced at least as satisfactorily as a more sophisticated model used previously.[69] More important, these calculations demonstrate that CD spectra of the nucleosides studied in terms of two vibronic transitions above 250 nm is in total conformity with current theoretical concepts.

Conclusions

We resolved the X band of the adenosine into three vibronic transitions and were able to specify the positions, dipole strengths, and moments of the two lower energy transitions. We have shown that, in terms of these quantities, a wholly self-consistent interpretation may be given to both isotropic and anisotropic spectra of adenine nucleosides and platinum complexes of adenosine. The results described set a definitive experimental framework against which the results of theoretical calculations may be tested and quantitatively evaluated.

Acknowledgment. This work was supported by the Australian Research Grants Committee.

(68) M. Sundaralingam, *J. Am. Chem. Soc.*, **93**, 6644 (1971).

(69) D. W. Miles, W. H. Inskeep, L. R. Townsend, and H. Eyring, *Jerusalem Symp. Quantum. Chem. Biochem.*, **4**, 325 (1972).

The Oxygen Analogue of the Protonated Cyclopropane Problem. A Theoretical Study of the $C_2H_5O^+$ Potential Energy Surface[1]

Ross H. Nobes, William R. Rodwell, Willem J. Bouma, and Leo Radom*

Contribution from the Research School of Chemistry, Australian National University, Canberra, A.C.T. 2600, Australia. *Received August 6, 1980*

Abstract: Ab initio molecular orbital theory has been used to study the $C_2H_5O^+$ potential surface. Calculations have been carried out with basis sets up to the size of double-ζ plus polarization (6-31G^{++}) and with electron correlation incorporated at the levels of second (MP2) and third (MP3) order Møller–Plesset perturbation theory. Direct gradient techniques have been used to locate minima (corresponding to stable isomers) and saddle points (corresponding to transition structures) in the surface. Results at the various levels of theory are compared. The calculations predict that the most stable $C_2H_5O^+$ isomer is the 1-hydroxyethyl cation (**11**). Apart from the other experimentally observed isomers, viz., the methoxymethyl cation (**9**) and O-corner-protonated oxirane (**7**), the calculations predict that vinyloxonium ($CH_2CHOH_2^+$) (**12**) is also likely to be experimentally observable because of its low relative energy and high barrier to intramolecular rearrangement. O-Corner-protonated oxirane (**7**) is the only protonated oxirane structure which is found to be a minimum in the $C_2H_5O^+$ surface. Face-, edge-, and C-corner-protonated structures collapse without activation to other isomers. Likewise, the ethoxy cation ($CH_3CH_2O^+$) (**16**) and the 2-hydroxyethyl cation ($HOCH_2CH_2^+$) (**10**) are predicted not to be stable species.

Introduction

The structure of protonated cyclopropane is a subject which has aroused considerable experimental[2] and theoretical[3] interest. All calculations reported to date agree that the face-protonated form (**1**) lies considerably higher in energy than the edge (**2**)- and corner (**3**)-protonated structures. The most reliable calculations,[3f] carried out at the CEPA-PNO/DZP level on STO-3G optimized geometries, find the edge-protonated structure to lie lower in energy (by ~20 kJ mol^{-1}) than corner-protonated cyclopropane and to lie about 10 kJ mol^{-1} higher than the isopropyl cation, the lowest energy $C_3H_7^+$ isomer.

(1) Presented in part at (a) The Australian Conference on Molecular Physics and Quantum Chemistry, Sydney, February, 1980; (b) The 6th National Conference of the Royal Australian Chemical Institute, Division of Organic Chemistry, Melbourne, August 1980.

(2) (a) Collins, C. J. *Chem. Rev.* **1969**, *69*, 541. (b) Lee, C. C. *Prog. Phys. Org. Chem.* **1970**, *7*, 129. (c) Fry, J. L.; Karabatsos, G. J. In "Carbonium Ions"; Olah, G. A., Schleyer, P. v. R., Ed.; Interscience: New York, 1970; Vol. 2, Chapter 14. (d) Saunders, M.; Vogel, P.; Hagan, E. L.; Rosenfeld, J. *Acc. Chem. Res.* **1973**, *6*, 53. (e) Brouwer, D. M.; Hogeveen, H. *Prog. Phys. Org. Chem.* **1972**, *9*, 179. (f) Chong, S. L.; Franklin, J. L. *J. Am. Chem. Soc.* **1972**, *94*, 6347. (g) McAdoo, D. J.; McLafferty, F. W.; Bente, P. F. *Ibid.* **1972**, *94*, 2027. (h) Dymerski, P. P.; Prinstein, R. M.; Bente, P. F.; McLafferty, F. W. *Ibid.* **1976**, *98*, 6834.

(3) (a) Radom, L.; Poppinger, D.; Haddon, R. C. in "Carbonium Ions"; Olah, G. A., Schleyer, P. v. R., Ed.; Interscience: New York, **1976**; Vol. 5, Chapter 38. (b) Radom, L.; Pople, J. A.; Buss, V.; Schleyer, P. v. R. *J. Am. Chem. Soc.* **1972**, *94*, 311. (c) Bodor, N.; Dewar, M. J. S.; Lo, D. H. *Ibid.* **1972**, *94*, 5303. (d) Hariharan, P. C.; Radom, L.; Pople, J. A.; Schleyer, P. v. R. *Ibid.* **1974**, *96*, 599. (e) Bischof, P. K.; Dewar, M. J. S. *Ibid.* **1975**, *97*, 2278. (f) Lischka, H.; Kohler, H. J. *Ibid.* **1978**, *100*, 5297.

0002-7863/81/1503-1913$01.25/0 © 1981 American Chemical Society

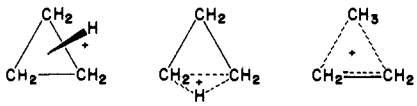

1 2 3

In this paper, we examine the much less studied oxygen analogue of protonated cyclopropane, namely, protonated oxirane. An attempt is made to answer several fundamental questions concerning this system. (i) What is the lowest energy structure of protonated oxirane? (ii) What is the status (i.e., local minimum, saddle point, nonstationary point, etc.) in the $C_2H_5O^+$ surface of structures corresponding to face (**4**)-, C···C edge (**5**)-, C···O edge (**6**)-, O-corner (**7**)-, and C-corner (**8**)-protonated oxiranes? (iii) What is the relationship in the $C_2H_5O^+$ surface of the protonated oxiranes to open-chain isomers such as the methoxymethyl cation (**9**), the 2-hydroxyethyl cation (**10**), the 1-hydroxyethyl cation (**11**), vinyloxonium (**12**), the carbenoid isomers **13**–**15**, and the ethoxy cation (**16**)? The technique used to tackle these questions is ab initio molecular oribital theory. Gradient techniques are used to characterize directly minima (corresponding to stable isomers) and saddle points (corresponding to transition structures separating the stable isomers) in the potential surface.

Method and Results

Standard self-consistent-field molecular orbital calculations were initially carried out by using a modified version[4a] of the Gaussian 70 system of programs.[4b] Minima and saddle points were obtained for all species by using gradient optimization techniques[5] and the minimal STO-3G[6] basis set. For completely asymmetric structures, such optimizations involved 18 degrees of freedom. In some instances the number of independent parameters was reduced through well-defined and specified symmetry constraints. Single energy calculations with the split-valence 4-31G[7] basis set at the STO-3G optimized geometries were also carried out and are denoted 4-31G//STO-3G.

For the 12 most interesting structures, reoptimization with the 4-31G basis set was performed and additional calculations were carried out in order to investigate the effects of increased basis set size and of electron correlation on the predicted relative energies. Two basis sets were used for these calculations, namely, the 6-31G basis of Hehre et al.[8] and a basis (6-31G^{++}) formed from this by the addition of d (5-component) and p polarization functions as for the 6-31G** basis set,[9] except that polarization function exponents optimized for correlated[10] rather than SCF wave functions were used. We note that in calculations[3f,11,12] on related series of molecules, p polarization functions on hydrogen as well as d functions on the heavy atoms have been found to be of importance.

The effects of valence electron correlation have been incorporated at the levels of second (MP2) and third (MP3) order Møller–Plesset perturbation theory.[10,13] Calculations at both levels were performed by using the 6-31G basis set, but computational expense dictated that the 6-31G^{++} calculations be restricted to second order. Previous work[14] on intramolecular rearrangements

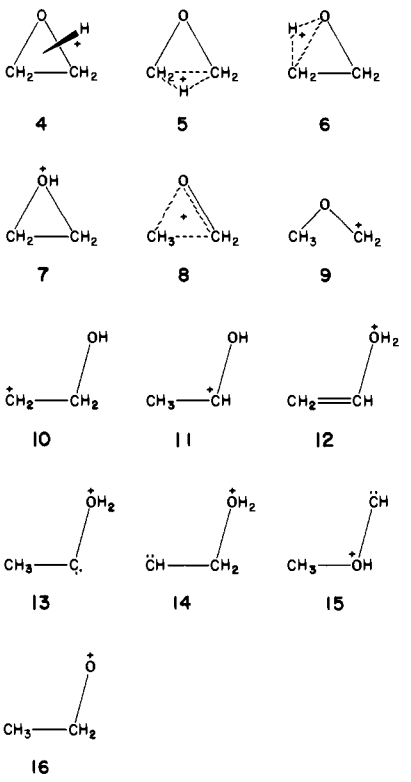

4 5 6 7 8 9 10 11 12 13 14 15 16

Figure 1. Possible isomeric $C_2H_5O^+$ structures.

in smaller systems has indicated that relative molecular energies including electron correlation up to third order of Møller–Plesset perturbation theory are in good agreement (~5 kJ mol^{-1}) with results of full coupled-cluster calculations, so that for these systems at least we regard the MP3 method as a reliable means of taking account of the effect of electron correlation on energy differences. For the 6-31G^{++} basis set, we have estimated the MP3 results by adding to the relative energies obtained from the MP3/6-31G calculations the difference between the 6-31G and 6-31G^{++} relative energies obtained at the MP2 level. This amounts to assuming that the effect on relative energies of basis set improvement is the same at the MP2 and MP3 levels. Evidence that this is a good approximation is provided by the results of ref 14 in which both MP2 and MP3 calculations are reported for polarized and unpolarized basis sets. Thus, if the MP3/4-31G relative energies of ref 14 are corrected as described above for the effect of improving the basis set from 4-31G to 6-31G*, then the mean absolute difference between the resulting estimated MP3/6-31G* relative energies and the directly calculated values is only 3 kJ mol^{-1} (maximum difference 8 kJ mol^{-1}). Such an error is certainly smaller than would be expected to remain in results from a full MP3/6-31G^{++} calculation (e.g., due to basis set deficiencies, incomplete treatment of electron correlation, inaccuracies in geometries), and we therefore regard this approach as an adequate approximation.

The 6-31G and 6-31G^{++} basis set SCF calculations were performed by using the ATMOL3 suite of programs,[15] the MP2 calculations by using a program developed in these laboratories,[16] and the MP3 calculations by using a rather extensively modified version[16] of Dykstra's SCEP program,[17] from which the MP3 energy can now be obtained, if desired, at the end of the first iterative cycle.

Optimized 4-31G structures (with STO-3G values of the structural parameters in parentheses) are displayed within the text. Corresponding total energies are shown in Table I. Relative

(4) (a) Hinde, A. L.; Nobes, R. H.; Poppinger, D.; Radom, L.; Vincent, M. A., unpublished results. (b) Hehre, W. J. et al. *QCPE* **1973**, *11*, 236.
(5) (a) Poppinger, D. *Chem. Phys. Lett.* **1975**, *34*, 332. (b) *Ibid.* **1975**, *35*, 550.
(6) Hehre, W. J.; Stewart, R. F.; Pople, J. A. *J. Chem. Phys.* **1969**, *51*, 2657.
(7) Ditchfield, R.; Hehre, W. J.; Pople, J. A. *J. Chem. Phys.* **1971**, *54*, 724.
(8) Hehre, W. J.; Ditchfield, R.; Pople, J. A. *J. Chem. Phys.* **1972**, *56*, 2257.
(9) Hariharan, P. C.; Pople, J. A. *Theor. Chim. Acta* **1973**, *28*, 213.
(10) Pople, J. A.; Binkley, J. S.; Seeger, R. *Int. J. Quantum Chem. Symp.* **1976**, *10*, 1.
(11) Bouma, W. J.; Radom, L.; Rodwell, W. R. *Theor. Chim. Acta* **1980**, *56*, 149.
(12) Rodwell, W. R.; Radom, L., unpublished data.
(13) Møller, C.; Plesset, M. S. *Phys. Rev.* **1934**, *46*, 618.
(14) Pople, J. A.; Krishnan, R.; Schlegel, H. B.; Binkley, J. S. *Int. J. Quantum Chem.* **1978**, *14*, 545.
(15) Saunders, V. R.; Guest, M. F. "ATMOL3 Users Guide"; Science Research Council: Daresbury, England.
(16) Rodwell, W. R., unpublished results.
(17) (a) Dykstra, C. E.; Schaefer, H. F.; Meyer, W. *J. Chem. Phys.* **1976**, *65*, 2740; (b) Dykstra, C. E. *QCPE* **1978**, *11*, 346. We thank Professor Dykstra for a prepublication version of this program.

Table I. Calculated Total Energies (Hartrees) for Stable Isomers and Transition Structures in the $C_2H_5O^+$ Potential Surface[a]

structure	STO-3G//STO-3G	4-31G//STO-3G	4-31G//4-31G	6-31G//4-31G
11	−151.32320	−152.98953	−152.99628	−153.15269
9	−151.30892	−152.96651	−152.97226	−153.12702
12	−151.28716	−152.97078	−152.97301	−153.12899
7	−151.29846	−152.93629	−152.94625	−153.10306
10	−151.23295	−152.92048	−152.93090	−153.08878
13	−151.22567	−152.88583		
14	−151.18803	−152.86740		
15	−151.21122	−152.86292		
17	−151.27212	−152.93015	−152.93832	−153.09470
5	−151.20966	−152.85441	−152.85881	−153.01608
6	−151.18872	−152.82436	−152.82741	−152.98412
19	−151.15887	−152.84982	−152.86011	−153.01606
20	−151.22322	−152.90965	−152.91949	−153.07745
21	−151.15946	−152.85309	−152.86067	−153.01687
22	−151.22878	−152.91285	−152.92683	−153.08438
23	−151.16110	−152.84174		
24	−151.13481	−152.81136		
25	−151.12269	−152.81866		
26	−151.11881	−152.78673		
27	−151.12208	−152.77316		

structure	MP2/6-31G// RHF/4-31G	MP3/6-31G// RHF/4-31G	RHF/6-31G**// RHF/4-31G	MP2/6-31G**// RHF/4-31G
11	−153.44234	−153.45480	−153.23595	−153.68447
9	−153.41902	−153.43009	−153.20686	−153.65359
12	−153.42046	−153.43649	−153.19038	−153.64253
7	−153.39683	−153.41021	−153.18179	−153.63665
10	−153.36308	−153.38100	−153.16333	−153.59716
17	−153.38031	−153.39534	−153.16337	−153.61287
5	−153.31552	−153.32979	−153.12414	−153.58284
6	−153.29336	−153.30526	−153.06587	−153.53818
19	−153.32554	−153.33587	−153.09074	−153.56432
20	−153.34954	−153.36759	−153.14958	−153.58034
21	−153.32402	−153.33394	−153.09298	−153.56391
22	−153.36852	−153.38479	−153.16869	−153.61266

[a] The notation "MP3/6-31G//RHF/4-31G", for example, means a third-order Møller–Plesset calculation with the 6-31G basis set on an RHF/4-31G optimized geometry.

Table II. Calculated Relative Energies (kJ mol^{-1}) for $C_2H_5O^+$ Isomers

	level[a]								
structure	A	B	C	D	E	F	G	H	I[b]
11	0	0	0	0	0	0	0	0	0
9	37.5	60.4	63.1	67.4	61.2	64.9	76.4	81.1	84.7
12	94.6	49.2	61.1	62.2	57.4	48.1	119.6	110.1	100.7
7	65.0	139.8	131.4	130.3	119.5	117.1	142.2	125.5	123.1
10	236.9	181.3	171.4	167.8	208.1	193.8	190.7	229.2	214.9
13	256.1	272.3							
14	354.9	320.6							
15	294.0	332.4							

[a] A ≡ RHF/STO-3G//RHF/STO-3G, B ≡ RHF/4-31G//RHF/STO-3G, C ≡ RHF/4-31G//RHF/4-31G, D ≡ RHF/6-31G//RHF/4-31G, E ≡ MP2/6-31G//RHF/4-31G, F ≡ MP3/6-31G//RHF/4-31G, G ≡ RHF/6-31G**//RHF/4-31G, H ≡ MP2/6-31G**//RHF/4-31G, I ≡ MP3/6-31G**//RHF/4-31G. [b] Estimated, see text.

Table III. Calculated Activation Energies (kJ mol^{-1}) for Rearrangements Linking $C_2H_5O^+$ Isomers

rearrangement	transition structure	level[a] A	B	C	D	E	F	G	H	I
7 → 7'	17	69.2	16.1	20.8	21.9	43.4	39.0	48.4	62.4	58.1
9 → 9'	**5**	260.6	294.3	297.9	291.3	271.7	263.3	217.2	185.8	177.3
7 → 9	6	288.1	293.9	312.0	312.3	271.7	275.5	304.3	258.5	262.4
12 → 11	19	336.8	317.6	296.4	296.5	249.2	264.2	261.6	205.3	220.3
10 → 7	**20**	25.5	28.4	30.0	29.7	35.5	35.2	36.1	44.2	43.8
10 → 12	**21**	192.9	176.9	184.4	188.8	102.6	123.6	184.7	87.3	108.3
10 → 11	**22**	10.9	20.0	10.7	11.6	0	0	0	0	0
13 → 12	**23**	169.5	115.8							
13 → 11	**24**	238.5	195.5							
14 → 12	**25**	171.5	128.0							
15 → 9	**26**	242.6	200.0							
15 → 7	**27**	234.0	235.7							

[a] See footnotes to Table II.

Table IV. Calculated Heats of Reaction (kJ mol^{-1}) for Rearrangements Linking $C_2H_5O^+$ Isomers

	level[a]								
rearrangement	A	B	C	D	E	F	G	H	I
7 → 9	−27.5	−79.3	−68.3	−62.9	−58.3	−52.2	−65.8	−44.5	−38.4
12 → 11	−94.6	−49.2	−61.1	−62.2	−57.4	−48.1	−119.6	−110.1	−100.7
10 → 7	−172.0	−41.5	−40.3	−37.5	−88.6	−76.7	−48.5	−103.7	−91.8
10 → 12	−142.3	−132.1	−110.6	−105.6	−150.6	−145.7	−71.0	−119.1	−114.2
10 → 11	−236.9	−181.3	−171.7	−167.8	−208.1	−193.8	−190.7	−229.2	−214.9
13 → 12	−161.4	−223.0							
13 → 11	−256.1	−272.3							
14 → 12	−260.3	−271.4							
15 → 9	−256.5	−272.0							
15 → 7	−229.0	−192.6							

[a] See footnotes to Table II.

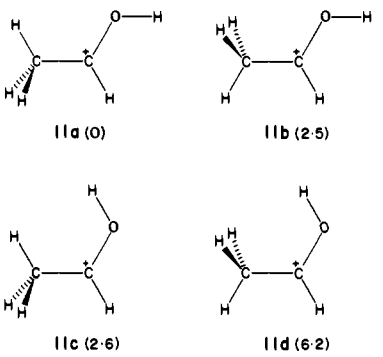

Figure 2. Relative energies (4-31G//STO-3G, kJ mol^{-1}) for conformations of the 1-hydroxyethyl cation (**11**).

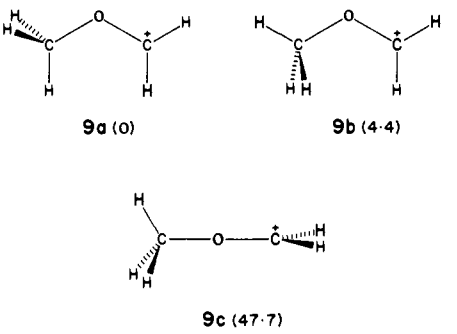

Figure 3. Relative energies (4-31G//STO-3G, kJ mol^{-1}) for conformations of the methoxymethyl cation (**9**).

energies of the stable isomers are listed in Table II while activation energies and heats of reaction are summarized in Tables III and IV, respectively.

Throughout this paper, bond lengths are given in angstroms and bond angles in degrees. Unless otherwise noted, all energy comparisons refer to MP3/6-31G^{++} values.

Discussion

Previous Work. Of the species examined in this study, the 1-hydroxyethyl cation (**11**), the methoxymethyl cation (**9**), and O-protonated oxirane (**7**) are well characterized experimentally as being distinct stable species.[18-35] Isomer **11** is generally believed to result from the fragmentation of primary and secondary alcohols and of various ethers and esters[18-24,27,28,31,32] and **9** to result from the fragmentation of alkyl methyl ethers.[19,20,23,24,28,29,31] Isomer **7** has been generated by a number of methods[23,25,26] but most directly[26] by protonation of oxirane at high pressure. There is no reliable evidence for the existence of other isomers shown in Figure 1. Theoretical calculations have recently been reported[36-40] for several of the ions under consideration in this paper. Experimental and theoretical results relevant to our study are discussed below.

1-Hydroxyethyl Cation (Protonated Acetaldehyde) (11). The 1-hydroxyethyl cation (**11**) is predicted to be the lowest energy $C_2H_5O^+$ isomer. STO-3G optimized structures were obtained for several conformations of this ion and 4-31G//STO-3G relative energies for these conformations are displayed in Figure 2. The best conformation (**11a**) has the methyl group eclipsed with respect

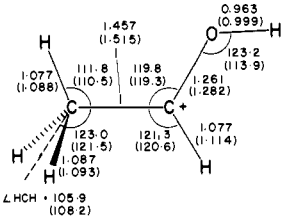

II

to the C–O bond (as in acetaldehyde itself) and HOCC trans. This conformation was re-optimized with the 4-31G basis set. The C–O bond is quite short, reflecting substantial double-bond character in accordance with contributions from the valence structures

$$CH_3-\overset{+}{C}H-\overset{\curvearrowleft}{O}H \leftrightarrow CH_3-CH=\overset{+}{O}H$$

Methoxymethyl Cation (9). Several conformations of the methoxymethyl cation (**9**) were examined and their structures optimized with the STO-3G basis set. Calculated 4-31G// STO-3G relative energies are shown in Figure 3. The preferred conformation has the methyl group eclipsed with respect to the adjacent C–O bond and was re-optimized with the 4-31G basis

(18) Van Raalte, D.; Harrison, A. G. *Can. J. Chem.* **1963**, *41*, 3118.
(19) Harrison, A. G.; Ivko, A.; Van Raalte, D. *Can. J. Chem.* **1966**, *49*, 1625.
(20) Shannon, T. W.; McLafferty, F. W. *J. Am. Chem. Soc.* **1966**, *88*, 5021.
(21) McLafferty, F. W.; Pike, W. T. *J. Am. Chem. Soc.* **1967**, *89*, 5951.
(22) Harrison, A. G.; Keyes, B. G. *J. Am. Chem. Soc.* **1968**, *90*, 5046.
(23) Beauchamp, J. L.; Dunbar, R. C. *J. Am. Chem. Soc.* **1970**, *92*, 1477.
(24) McLafferty, F. W.; Kornfeld, R.; Haddon, W. F.; Kevsen, K.; Sakai, I.; Bente, P. F.; Tsai, S. C.; Schuddemage, H. D. R. *J. Am. Chem. Soc.* **1973**, *95*, 3886.
(25) Staley, R. H.; Corderman, R. R.; Foster, M. S.; Beauchamp, J. L. *J. Am. Chem. Soc.* **1974**, *96*, 1260.
(26) Van de Graaf, B.; Dymerski, P. P.; McLafferty, F. W. *J. Chem. Soc., Chem. Commun.* **1975**, 978.
(27) Keyes, B. G.; Harrison, A. G. *Org. Mass Spectrom.* **1974**, *9*, 221.
(28) Lossing, F. P. *J. Am. Chem. Soc.* **1977**, *99*, 7526.
(29) Botter, R.; Pechine, J. M.; Rosenstock, H. M. *Int. J. Mass Spectrom. Ion Phys.* **1977**, *25*, 7.
(30) Yamdagni, R.; Kebarle, P. *J. Am. Chem. Soc.* **1976**, *98*, 1320.
(31) Solka, B. H.; Russell, M. E. *J. Phys. Chem.* **1974**, *78*, 1268.
(32) Refaey, K. M. A.; Chupka, W. A. *J. Chem. Phys.* **1968**, *48*, 5205.
(33) Hvistendahl, G.; Williams, D. H. *J. Am. Chem. Soc.* **1975**, *97*, 3097.
(34) Bowen, R. D.; Williams, D. H.; Hvistendahl, G. *J. Am. Chem. Soc.* **1977**, *99*, 7509.
(35) Bowen, R. D.; Williams, D. H.; Schwartz, H. *Angew. Chem., Int. Ed. Engl.* **1979**, *18*, 451.
(36) Catalan, J.; Yanez, M. *J. Am. Chem. Soc.* **1978**, *100*, 1398.
(37) Hopkinson, A. C.; Lien, M. H.; Csizmadia, I. G.; Yates, K. *Theor. Chim. Acta* **1978**, *47*, 97.
(38) Lischka, H.; Kohler, H. J. *Chem. Phys. Lett.* **1979**, *63*, 326.
(39) Alagona, G.; Scrocco, E.; Tomasi, J. *Theor. Chim. Acta* **1979**, *51*, 11.
(40) Farcasiu, D.; O'Donnell, J. J.; Wiberg, K. B.; Matturro, M. *J. Chem. Soc., Chem. Commun.* **1979**, 1124.

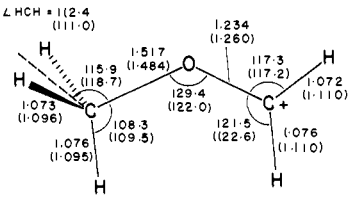

9

set. Again, the short C–O length reflects considerable electron delocalization

$$CH_3-\ddot{O}\sim\overset{+}{C}H_2 \leftrightarrow CH_3-\overset{+}{O}=CH_2$$

The barrier to in-plane inversion at oxygen is given by the relative energy of **9c**. The calculated barrier (47.7 kJ mol^{-1}) is in good agreement with an experimental value[40] (50 kJ mol^{-1}) determined in superacid solution and with a previous theoretical estimate.[40] **9** is found to lie 85 kJ mol^{-1} higher in energy than **11** which compares well with an experimental estimate of 75–82 kJ mol^{-1} based on the $\Delta H_f°$ values[28,29] for **11** (582 kJ mol^{-1}) and **9** (657–664 kJ mol^{-1}).

Vinyloxonium (Protonated Vinyl Alcohol) (12). The structure of this isomer was optimized with a C_s (planar) symmetry constraint. Its energy, 101 kJ mol^{-1} above **11**, is relatively low, but

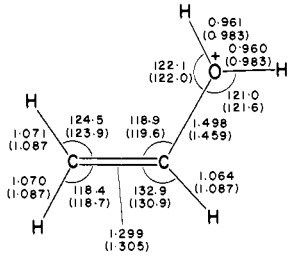

12

no experimental observation of this ion has yet been reported. We are unaware of any previous theoretical study of this ion.

O-Protonated Oxirane (7). The only protonated oxirane structure which we find to be a local minimum in the $C_2H_5O^+$ surface is O-protonated oxirane (7) whose structure was fully

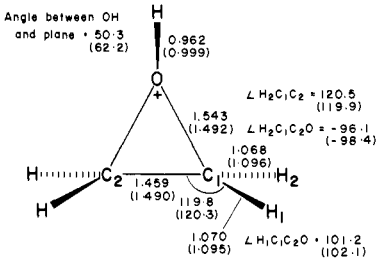

7

optimized subject only to a C_s symmetry constraint. The most widely accepted value of $\Delta H_f°$ for **7** appears to be that of Beauchamp (707 kJ mol^{-1})[25] which yields an energy for **7** relative to **11** of 125 kJ mol^{-1}. This may be compared with our best estimate of 123 kJ mol^{-1} and a previous theoretical estimate[38] of 122 kJ mol^{-1}.

If the O–H bond in **7** is constrained to lie in the plane of the ring, structure **17** is obtained with C_{2v} symmetry. This represents

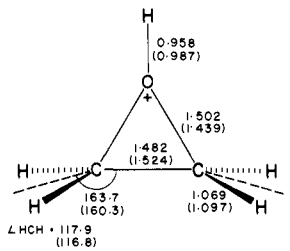

17

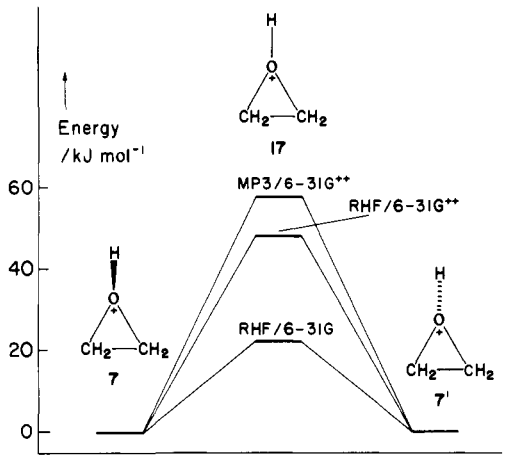

Figure 4. Schematic energy profile for inversion in O-protonated oxirane (**7**).

the transition structure for inversion in **7**, and the energy of **17** relative to **7** measures the inversion barrier (Figure 4). Our results (Table III and Figure 4) show that the calculated inversion barrier is strongly influenced by the presence of polarization functions in the basis set and by electron correlation. Our best value for the inversion barrier (58.1 kJ mol^{-1}) is therefore probably more reliable than previous theoretical estimates[37,38] which were obtained at lower levels of theory.

2-Hydroxyethyl Cation (10). The HOCC trans, OCCH-eclipsed conformation (**10**) of the 2-hydroxyethyl cation is found

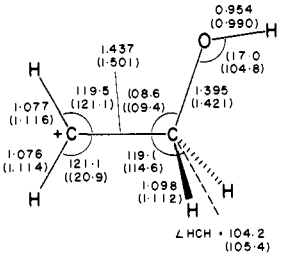

10

to be a genuine minimum on the STO-3G and 4-31G potential surfaces for $C_2H_5O^+$. The force constant matrix for this structure has, as required, all positive eigenvalues. We should note at this stage, however, that this appears not to be the case at higher levels of theory (see below). **10** is predicted to lie 215 kJ mol^{-1} above **11**. No reliable experimental information is available for this species.

A second conformation (**18**) of the hydroxyethyl cation is found

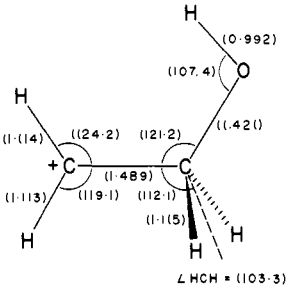

18

to be a transition structure for rotation about the C–O bond. Its energy relative to **10** is 40 kJ mol^{-1} (4-31G//STO-3G).[41] Conformations in which the CH_2^+ plane is perpendicular to CCO collapse without activation to **7**.

Carbenoid Isomers of $C_2H_5O^+$ (13–15). Three carbenoid isomers of $C_2H_5O^+$ were examined. Each was optimized subject to

(41) Calculated total energies for **18** are −151.21944 (STO-3G//STO-3G) and −152.90508 (4-31G//STO-3G) hartrees.

a C_s symmetry constraint and tested for stability with respect to C_1 distortions, yielding the STO-3G optimized structures shown in **13–15**.[42] All three isomers were found to have quite high

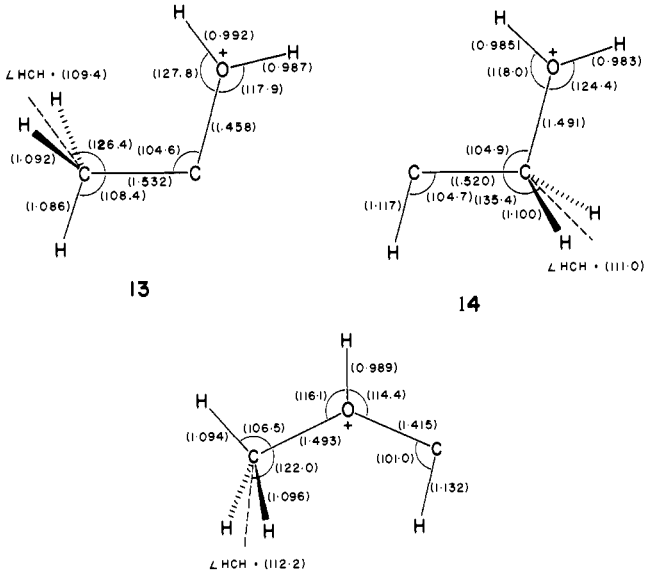

relative energies (270–330 kJ mol^{-1} above **11** with 4-31G//STO-3G) and for this reason were not examined further with the higher levels of theory used for the other isomers.

Ethoxy Cation (16). This was found not to represent a local minimum in the $C_2H_5O^+$ surface. Optimizations from structures of this type lead to collapse to the methoxymethyl cation (**9**) or to the 1-hydroxyethyl cation (**11**). Neither ion cyclotron resonance[23] nor collisional activation[24] studies find any evidence for a structure of the type **16**. On the other hand, it has been proposed[43] that **16** is indeed the species formed from $CH_3CH_2O^-$ in a charge reversal experiment.

C···C Edge-Protonated Oxirane (5). The Degenerate 1,3-Hydrogen Shift 9 → 9′. Our calculations show that C···C edge-protonated oxirane (**5**), with C_{2v} symmetry, is a saddle point in

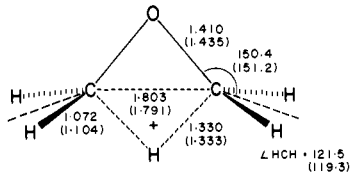

the $C_2H_5O^+$ surface. It represents the transition structure for the degenerate proton shift **9** → **9′** for which the schematic energy profile is shown in Figure 5. The predicted activation energy for this rearrangement is 177 kJ mol^{-1}. Experimental work[33] has shown that prior to decomposition of **9** via loss of CH_4 (requiring ~326 kJ mol^{-1}), all hydrogen atoms have become equivalent. Measurements[33] on the analogous rearrangement in the $C_3H_7O^+$ system yield an activation energy of ≳243 kJ mol^{-1}. Hence it has been proposed[33] that the rearrangement **9** → **9′** requires between ~243 and ~326 kJ mol^{-1}. Another independent estimate,[44] arising from ICR studies, puts the barrier at 220 kJ mol^{-1}. The reaction **9** → **5** → **9′** is a 1,3-sigmatropic shift. Sizable barriers have previously been found for such rearrangements in related systems.[45-48]

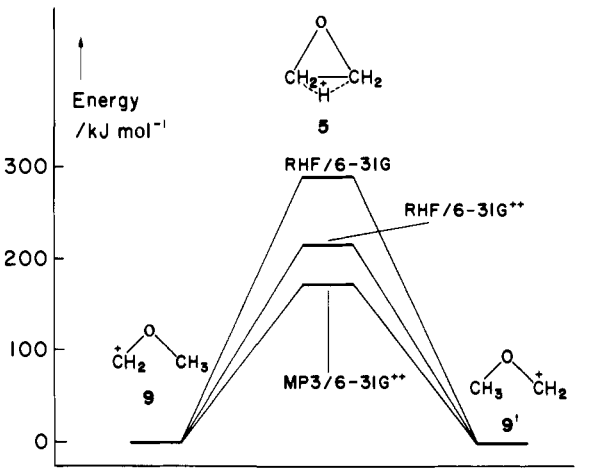

Figure 5. Schematic energy profile for the degenerate 1,3-hydrogen shift in the methoxymethyl cation (**9**).

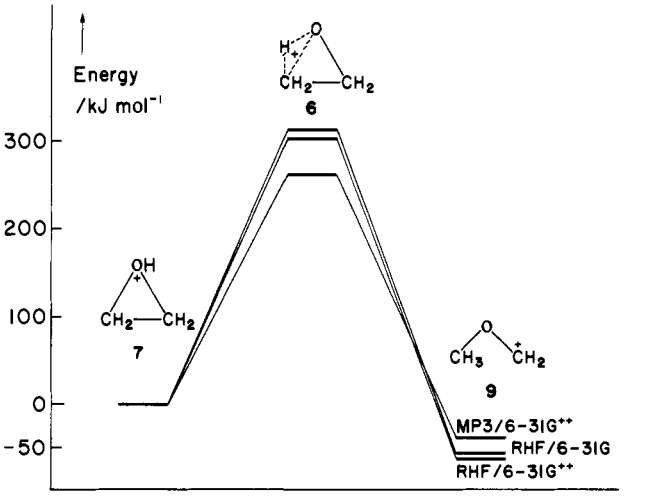

Figure 6. Schematic energy profile for the rearrangement of O-protonated oxirane (**7**) to the methoxymethyl cation (**9**).

C···O Edge-Protonated Oxirane (6). The Rearrangement of O-Protonated Oxirane (7) to the Methoxymethyl Cation (9). The saddle point linking O-protonated oxirane (**7**) and the methoxymethyl cation (**9**) (Figure 6), determined with no symmetry constraints, has a C···O edge-protonated oxirane structure (**6**).

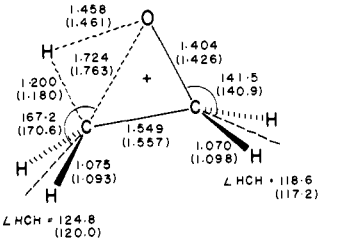

Our best calculated barrier to the rearrangement of **7** to **9** is 262 kJ mol^{-1}. No previous theoretical studies of this rearrangement have been reported. There exists conclusive experimental evidence based on metastable peak shapes,[20] dissociation energies for CH_4 loss,[34] and labeling studies[18,27,33,34] that **9** reacts over a potential energy profile distinct from that over which **7** and **11** react, i.e.,

(42) Isomer **15** was also optimized with HOCH cis, yielding a 4-31G//STO-3G energy 1.4 kJ mol^{-1} higher than that of the HOCH trans isomer.

(43) Bursey, M. M.; Hass, J. R.; Harvan, D. J.; Parker, C. E. *J. Am. Chem. Soc.* **1979**, *101*, 5485.
(44) van Doorn, R.; Nibbering, N. M. M. *Org. Mass Spectrom.* **1978**, *13*, 527.
(45) Bouma, W. J.; Poppinger, D.; Radom, L. *J. Am. Chem. Soc.* **1977**, *99*, 6443.
(46) Bouma, W. J.; Vincent, M. A.; Radom, L. *Int. J. Quantum Chem.* **1978**, *14*, 767.
(47) Rodwell, W. R.; Bouma, W. J.; Radom, L. *Int. J. Quantum Chem.* **1980**, *18*, 107.
(48) Adeney, P. D.; Bouma, W. J.; Radom, L.; Rodwell, W. R. *J. Am. Chem. Soc.* **1980**, *102*, 4069.

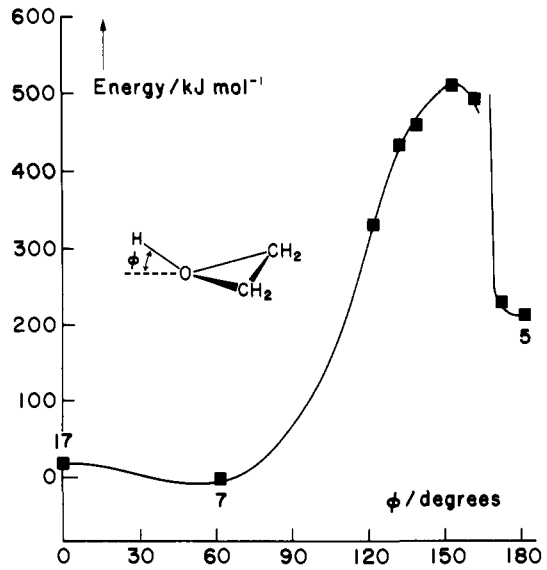

Figure 7. Schematic reaction profile (4-31G//STO-3G) connecting face-protonated oxirane (**4**) with O-corner-protonated (**7**) and C···C edge-protonated oxirane (**5**).

that the barrier separating **9** from **7** and **11** is high. This is consistent with our result. Williams et al.[34] have estimated a barrier of 340 kJ mol^{-1} for the rearrangement of **7** to **9** via an alternative C–C bond homolysis mechanism.

C-Corner-Protonated Oxirane (8). This structure is not a stationary point in the $C_2H_5O^+$ surface. It collapses without activation to the methoxymethyl cation (**9**).

Face-Protonated Oxirane (4). This structure also does not correspond to a stationary point in the $C_2H_5O^+$ surface. Calculations, carried out as a function of the out-of-plane angle ϕ of the O–H bond (with optimization of the remaining parameters), yield the energy profile of Figure 7. This shows that collapse occurs either to O-protonated oxirane (**7**) or to the C···C edge-protonated form (**5**) which would subsequently rearrange to **9**.

The Rearrangement of Protonated Vinyl Alcohol (12) to Protonated Acetaldehyde (11). The transition structure (**19**) for this

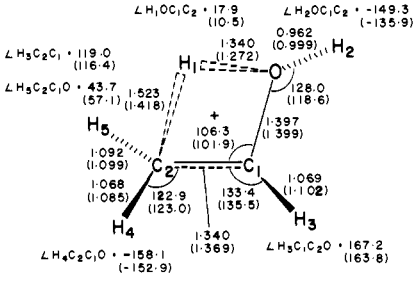

19

1,3-sigmatropic hydrogen shift (Figure 8) has no symmetry. The structure of **19** is very similar to that determined[45-47] for the corresponding rearrangement in the parent unprotonated system, vinyl alcohol → acetaldehyde. Comparison of results for these two rearrangements also shows that protonation has the effect, first, of increasing the exothermicity and, second, of decreasing the activation energy for the vinyl alcohol → acetaldehyde rearrangement. Our results indicate that protonated vinyl alcohol is a relatively low-energy species with a high barrier to rearrangement to **11** and is therefore likely to be experimentally observable. The high barrier is consistent with labeling studies[34] which show that the hydroxyl hydrogen in ions generated initially as **11** remains attached to oxygen up to dissociation to acetylene + H_3O^+.

The Rearrangement of the 2-Hydroxyethyl Cation (10) to O-Corner-Protonated Oxirane (7). The transition structure for the rearrangement **10** → **7** (Figure 9) is again completely asymmetric. In addition, the 2-hydroxyethyl cation (**10**) lies in a

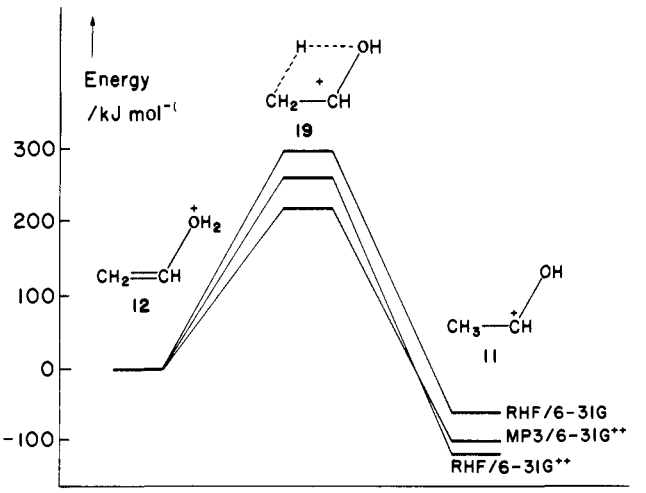

Figure 8. Schematic energy profile for the rearrangement of protonated vinyl alcohol (**12**) to protonated acetaldehyde (**11**).

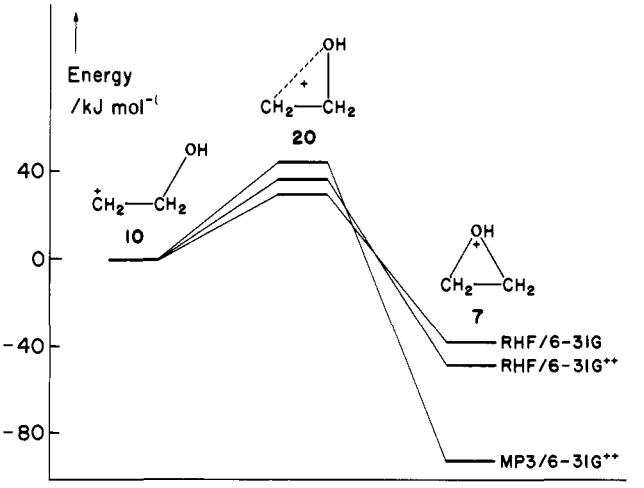

Figure 9. Schematic energy profile for the rearrangement of the 2-hydroxyethyl cation (**10**) to O-corner-protonated oxirane (**7**).

relatively shallow well on the STO-3G and 4-31G surfaces. Nevertheless, we were able to obtain rigorously transition structures (**20**) on both surfaces. Our best calculated activation

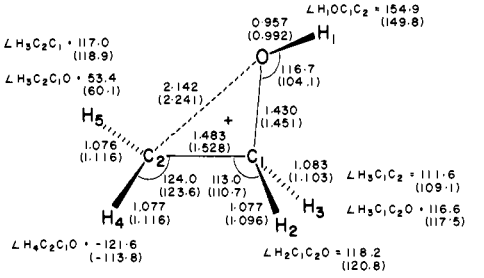

20

energy for **10** → **7** is 44 kJ mol^{-1}. A considerably larger estimate of 105 kJ mol^{-1} was obtained[37] in a previous more approximate treatment. Rapid and reversible rearrangement of **11** to **7** via a structure resembling **10** has been proposed[34] to account for results of labeling experiments,[18,27,33] and the barrier has been estimated[34] to be about 84 kJ mol^{-1} above **7**. Our corresponding calculated value is 135 kJ mol^{-1}.

The Rearrangement of the 2-Hydroxyethyl Cation (10) to Protonated Vinyl Alcohol (12). This rearrangement (Figure 10) also involves a transition structure (**21**) with no symmetry. The calculated activation energy is 108 kJ mol^{-1}.

The Rearrangement of the 2-Hydroxyethyl Cation (10) to the 1-Hydroxyethyl Cation (Protonated Acetaldehyde) (11). This rearrangement, via transition structure **22**, is found to require a

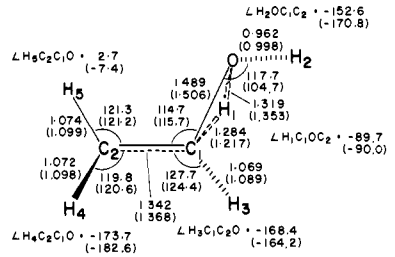

21

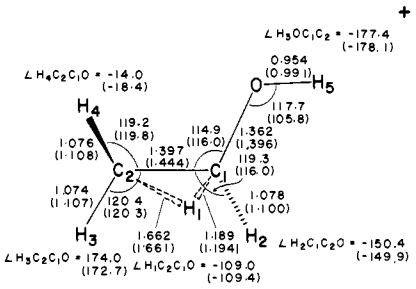

22

small activation energy on both the STO-3G and 4-31G surfaces. However, at higher levels of theory (i.e., with the inclusion of polarization functions in the basis set and incorporation of electron correlation), the energy of **22** drops below that of **10** (see Table I and Figure 11); i.e., **10** is predicted to collapse without activation to **11**. Thus, although the 2-hydroxyethyl cation is predicted to be stable with respect to cyclization to O-protonated oxirane (Figure 9) and with respect to a 1,2-proton shift to protonated vinyl alcohol (Figure 10), it is unlikely to be an observable species because of rearrangement by means of a 1,2-hydride shift to the 1-hydroxyethyl cation (Figure 11).

It is of interest that whereas transformation of **12** to **11** by means of a direct 1,3-sigmatropic shift is described by the reaction profile shown in Figure 8, an alternative pathway is provided by combining the results of Figures 10 and 11. This involves successive 1,2-hydrogen shifts, **12** → **10** → **11**, and a barrier of 223 kJ mol^{-1}, a value very close to that (220 kJ mol^{-1}) of the direct rearrangement.

Rearrangements Involving the Carbenoid Species 13–15. The remaining rearrangements, involving the carbenoid species **13–15**, were examined in somewhat less detail. Geometry optimizations were restricted to the STO-3G basis set and energy comparisons to the 4-31G//STO-3G level. Previous calculations[49] have shown that barriers to carbenoid rearrangements are lowered substantially by addition of polarization functions to the basis set and by incorporation of electron correlation. For this reason, we have carried out[50] higher level calculations on the prototype rearrangements (1) and (2).

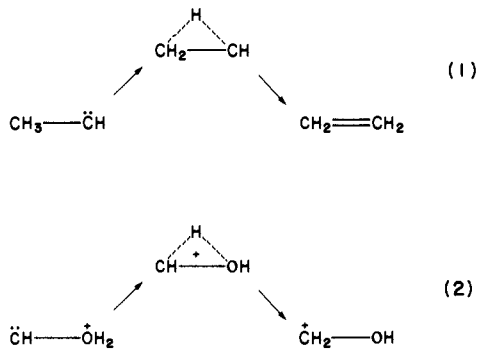

(1)

(2)

For (1), the activation energy is lowered from 83 kJ mol^{-1} at the 4-31G//4-31G level to 9 kJ mol^{-1} at MP3/6-31G^{++}// RHF/4-31G, while for (2) the corresponding lowering is from

(49) See, for example: Schaefer, H. F. *Acc. Chem. Res.* **1979**, *12*, 288.
(50) Nobes, R. H.; Rodwell, W. R.; Radom, L. *Chem. Phys. Lett.* **1980**, *74*, 269.

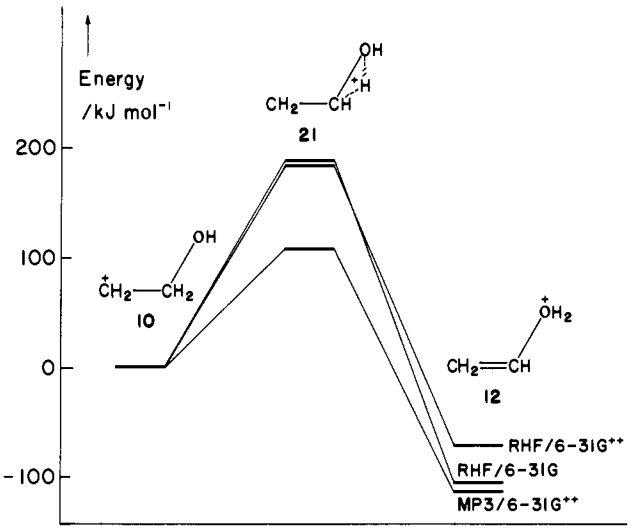

Figure 10. Schematic energy profile for the rearrangement of the 2-hydroxyethyl cation (**10**) to protonated vinyl alcohol (**12**).

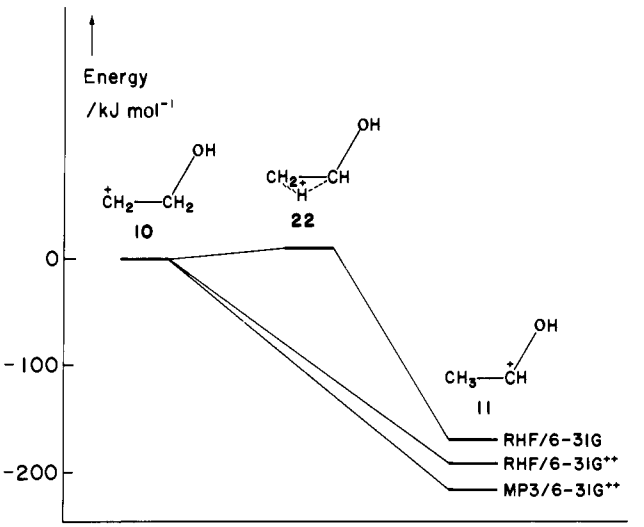

Figure 11. Schematic energy profile for the rearrangement of the 2-hydroxyethyl cation (**10**) to the 1-hydroxyethyl cation (protonated acetaldehyde) (**11**).

200 to 145 kJ mol^{-1}. It is likely that similar effects operate for the analogous rearrangements in the $C_2H_5O^+$ system and we have applied approximate corrections of 74 and 55 kJ mol^{-1}, respectively, to obtain improved estimates of the activation energies.

Isomer **13** may rearrange to protonated vinyl alcohol (**12**) by means of a 1,2-hydrogen shift via transition structure **23**. The

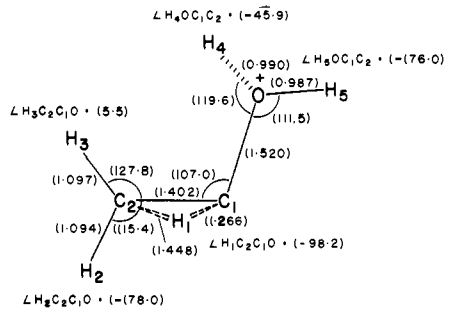

23

calculated barrier to rearrangement is 116 kJ mol^{-1} (4-31G// STO-3G) leading to a corrected value (as outlined above) of about 40 kJ mol^{-1}. Rearrangement of **13** to the most stable $C_2H_5O^+$ isomer, **11**, by means of a 1,2-proton shift and the transition structure **24** is predicted to require somewhat greater activation energy. The corrected calculated value is 140 kJ mol^{-1}.

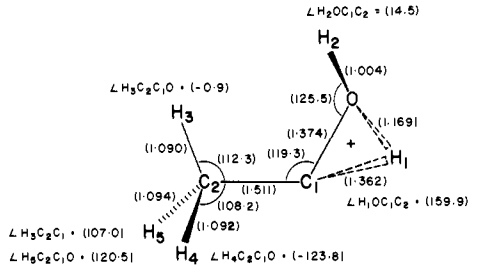

24

The 1,2-hydrogen shift which converts **14** to **12** via transition structure **25** has a corrected calculated activation energy of about 50 kJ mol^{-1}.

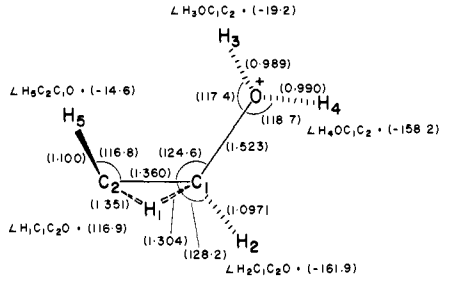

25

Finally, isomer **15** is separated by a 1,2-proton shift via transition structure **26** from the methoxymethyl cation (**9**). The

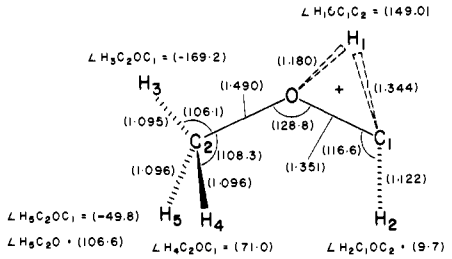

26

corrected activation energy is 145 kJ mol^{-1}. An alternative rearrangement of **15** to O-protonated oxirane (**7**) via **27** has a

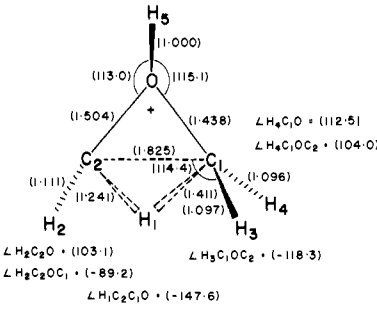

27

calculated activation barrier of 236 kJ mol^{-1} (4-31G//STO-3G). This would undoubtedly be lowered in a higher level treatment, but in the absence of data for a suitable model system, it is difficult to estimate the correction involved.

Our results suggest that of the 3 carbenoid isomers **13**–**15**, it is surprisingly the highest energy species **15** that offers the best prospect of experimental observation. Both **13** and **14** can undergo low-energy rearrangements to more stable isomers.

Comparison of Theoretical Levels. One of the aims of the present study has been to compare results at the various levels of theory and to attempt to assess the levels required to adequately describe potential surfaces and, in particular, transition structures.

We begin by noting that STO-3G-optimized geometries are frequently used in conjunction with energy calculations at higher levels of theory in order to obtain relative energies of stable molecules. This is generally a satisfactory and economical approximation. On the other hand, little information is available on the use of this approach for estimating activation energies so it is useful to comment on this point here.

Examination of columns B and C of Table III shows that there are six rearrangements for which we have activation energies calculated with both STO-3G- and 4-31G-optimized geometries. The mean absolute deviation between the activation energies for these rearrangements calculated with STO-3G-optimized geometries (i.e., 4-31G//STO-3G) and the full 4-31G//4-31G results is just 10 kJ mol^{-1} (with a maximum difference of 21 kJ mol^{-1}). A likely situation in which this approach might be expected to break down is when the energy of product relative to reactant is poorly described by the STO-3G basis set. In this study, this is true for the energy of **10** relative to **7** which is 172 kJ mol^{-1} with STO-3G//STO-3G and 40 kJ mol^{-1} with 4-31G//4-31G. Under these circumstances, we might expect, as a consequence of the Hammond postulate,[51] that the transition structure for the transformation **10** → **7** resembles **10** to a much greater extent in the STO-3G than in the 4-31G surface. As a consequence, the use of the STO-3G transition structure in conjunction with the 4-31G basis set (4-31G//STO-3G) might be a poor approximation to the full 4-31G//4-31G result. As it turns out, even for this rearrangement, this is not the case. The activation energies for the rearrangement **10** → **7** via **13** are 28 (4-31G//STO-3G) and 30 (4-31G//4-31G) kJ mol^{-1}.

Thus, for the systems examined in this paper at least, we find that use of STO-3G optimized geometries is a satisfactory approximation. We have reached a similar conclusion in previous studies of 1,3-sigmatropic rearrangements.[47,48] Nevertheless, because the 4-31G structures are available and are likely to be the more accurate, we have used these exclusively in the higher level calculations of this study.

At higher levels of theory, both the effect of addition of polarization functions to the basis set (6-31G → 6-31G^{++}) and of incorporation of electron correlation (RHF → MP2, MP3) are of interest. For the stable isomers, the most striking variation occurs for the energy of protonated vinyl alcohol (**12**) relative to that of protonated acetaldehyde (**11**). This increases markedly (from 62 to 120 kJ mol^{-1}) in going from 6-31G to 6-31G^{++} and comes back slightly (to 101 kJ mol^{-1}) with MP3. A qualitatively similar but quantitatively much smaller effect is observed[11] for the comparison of the unprotonated neutrals, vinyl alcohol and acetaldehyde.

The calculated inversion barrier in protonated oxirane (Figure 5) is found to be sensitive to the level of calculation. Both polarization functions and electron correlation lead to a substantial lowering in barrier height.

For the rearrangement reactions (Figures 6, 7, 9–12), the calculated activation barriers generally decrease both in going to 6-31G^{++} and MP3 although the relative magnitudes of these two changes vary from system to system. In the case of **10** → **11**, this is sufficient to remove the barrier completely. For the degenerate shift **9** → **9′**, the RHF/6-31G barrier of 291 kJ mol^{-1} is reduced to 177 kJ mol^{-1} with MP3/6-31G^{++}.

Finally, we note that for the 11 comparisons available in Tables II and III 6-31G results are very close to 4-31G and MP3 results close to MP2. The mean absolute difference between the 6-31G and 4-31G relative energies is 2 kJ mol^{-1} with a maximum difference of 4 kJ mol^{-1}. The mean absolute difference between the MP3 and MP2 relative energies is 8 kJ mol^{-1} with a maximum difference of 15 kJ mol^{-1}.

Conclusions

Several important conclusions emerge from this study.

(i) There are four energetically low-lying stable isomers of $C_2H_5O^+$.

(ii) In addition to those isomers that have been previously observed experimentally (namely, the 1-hydroxyethyl cation (**11**), the methoxymethyl cation (**9**), and O-protonated oxirane (**7**)),

(51) Hammond, G. S. *J. Am. Chem. Soc.* **1955**, *77*, 334.

vinyloxonium (**12**) is indicated to be a relatively low-energy species separated from **11** by a substantial barrier to intramolecular rearrangement and is therefore an attractive prospect for experimental observation.

(iii) The only stable form of protonated oxirane is the O-corner-protonated isomer (**7**).

(iv) Although the 2-hydroxyethyl cation (**10**) is stable with respect to cyclization to O-protonated oxirane (**7**) and proton migration to vinyloxonium (**12**), it collapses without activation energy to the 1-hydroxyethyl cation (**11**).

(v) The ethoxy cation (**16**) is also indicated to be an unstable species, collapsing without activation to **9** or **11**.

(vi) STO-3G optimized structures are found to provide a reasonable basis for calculating activation energies at higher levels of theory.

(vii) Both polarization functions and electron correlation are found to be important in providing an accurate description of the $C_2H_5O^+$ potential energy surface.

Acknowledgment. We thank Mr. M. A. Ballard for assistance with some of the calculations. We are indebted to Dr. Dudley Williams for helpful and stimulating discussions.

An Investigation of the Mechanism of Phosphine Photolysis

J. P. Ferris*[1] and Robert Benson

Contribution from the Department of Chemistry, Rensselaer Polytechnic Institute, Troy, New York 12181. *Received June 11, 1980*

Abstract: Photolysis of PH_3 gives P_2H_4 as an initial photoproduct. The concentration of P_2H_4 increases to a maximum and then decreases during the course of the photolysis. Disproportionation of PH_2 was eliminated as a reaction by the observation that the ratio of $4n_{P_4}/n_{P_2H_4}$ extrapolates to near zero at zero reaction time. The yield of P_2H_4 increases with increasing PH_3 concentration, but it is only slightly affected by the addition of SF_6 or N_2. The absence of an effect with the added inert gases eliminates the possibility of termolecular reactions and hot atom reactions in the formation of P_2H_4. P_2H_4 formation from PH_2 was shown to be a gas phase and not a wall reaction by flash photolysis studies. The pseudo-second-order rate constant determined for the formation of P_2H_4 ($(5.4 \pm 2.4) \times 10^9$ M^{-1} s^{-1}) is diffusion controlled and close to the rate constant for the formation of N_2H_4 from NH_2. That the rate constants are comparable suggests both hydrides are formed by the same reaction pathway. Initial quantum yields are Φ_{PH_3} (PH_3 loss) = 1.78 ± 0.18, $\Phi_{H_2} = 0.43 \pm 0.23$, $\Phi_{P_2H_4} = 0.80 \pm 0.08$, and $\Phi_{4P_4} = 0.04 \pm 0.16$. The value of Φ_{PH_3} close to 2 indicates the formation of PH_2 by reaction of H and PH_3 (reaction 3) is an important reaction pathway in PH_3 photolysis. A new mechanism is proposed for PH_3 photolysis, and the significance of these findings to the atmospheric chemistry of Jupiter is discussed.

Phosphine (PH_3) photochemistry has been studied sporadically since the initial work of Melville in 1932,[2] but these limited studies are dwarfed by the extensive investigations of NH_3, the corresponding group 5 hydride.[3] The apparent lack of interest in PH_3 may reflect the hazardous nature of the compound[4] as well as the experimental problem of having a solid photoproduct, P_4, coat the walls of the photolysis cell; neither of these problems complicates the study of NH_3 photochemistry. The discovery of PH_3 in the atmospheres of Jupiter and Saturn by Ridgway,[5] a result which has subsequently been confirmed by airborne observations,[6] ground-based studies,[7] and the Voyager II mission,[8] has prompted increased interest in PH_3 photochemistry. The discovery of PH_3 led to the suggestion that the red coloration of the Great Red Spot of Jupiter is due to the photolysis of PH_3 to red phosphorus (P_4).[9] The PH_3 may be formed from phosphorus in the lower, hotter levels of the Jovian atmosphere or by reaction with H atoms in the upper atmosphere or with the NH_3–H_2O clouds in the upper troposphere.[10]

The primary process in the photolysis of PH_3 between 160 and 210 nm is predissociation to PH_2 and H atoms (eq 1)[11] which is

$$4PH_3 \xrightarrow{h\nu} P_4 + 6H_2 \qquad (1)$$

reflected in the featureless UV spectrum of PH_3 from 240 nm down to the vacuum ultraviolet.[12] Red phosphorus and H_2 are the only photoproducts that have been reported (eq 1).[2,13]

The quantum yield for PH_3 loss (Φ_{PH_3}) was reported to be 0.5[2] and was not affected by pressure variations of 10–760 torr and temperature variations of 15–300 °C. The Φ_{PH_3} increased with an increase in the surface to volume ratio of the reaction cell. This finding suggests that the secondary reactions of H and PH_2 occurred on the wall of the reaction vessel and that their activation energies were small. One of the proposed secondary reactions, the recombination of H and PH_2 (reaction 8), would account for a value of Φ_{PH_3} less than 1.

H atoms have been demonstrated to have an important role in the decomposition of PH_3.[14] They react with PH_3 to give the same products, H_2 and P_4, as are observed in the photolysis of PH_3. The rate constant for the reaction of H atoms with PH_3

(1) To whom correspondence should be addressed.
(2) Melville, H. *Proc. R. Soc. London, Ser. A* **1932**, *138*, 374–395. *Ibid.* **1933**, *139*, 541–557.
(3) Noyes, W. A., Jr.; Leighton, P. A "The photochemistry of Gases"; Dover Publications: New York, 1966.
(4) Mellor, J. W. "Comprehensive Treatise of Inorganic and Theoretical Chemistry"; Longmans, Green and Co., New York, 1928; Vol. III, pp 802–822.
(5) Ridgway, S. T. *Astrophys. J.* **1974**, *187*, L41–L43. *Ibid.* **1974**, *192*, L51. Ridgway, S. T.; Wallace, L.; Smith, G. R. *Astrophys. J.* **1976**, *207*, 1002–1006.
(6) Larson, H. P.; Treffers, R. R.; Fink, U. *Astrophys. J.* **1977**, *211*, 972–979.
(7) Bregman, J. D.; Lester, D. F.; Rank, D. M. *Astrophys. J.* **1975**, *202*, L55–L56.
(8) Hanel, R.; Conrath, B.; Flaser, M.; Herath, L.; Kunde, U.; Lowman, P.; Maguire, W.; Pearl, J.; Pirraglia, J.; Samuelson, R.; Gautier, D.; Horn, L.; Kumar, S.; Ponnamperuma, C. *Science (Washington, D.C.)* **1979**, *206*, 952–956.
(9) Prinn, R. G.; Lewis, J. S. *Science (Washington, D.C.)* **1975**, *190*, 274–276.
(10) Howland, G. R.; Harteck, P.; Reeves, R. R., Jr. *Icarus* **1979**, *37*, 301–306.
(11) DiStefano, G.; Lenzi, M.; Margani, A.; Mele, A.; Xuan, C. N. *J. Photochem.* **1977**, *7*, 335–344.
(12) Kleg, D.; Welge, K. H. *Z. Naturforsch., A* **1965**, *20A*, 124–131.
(13) Norrish, R. G.; Oldershaw, G. A. *Proc. R. Soc. London, Ser. A* **1961**, *262*, 1–9.
(14) Wiles, D. M.; Winkler, C. A. *J. Phys. Chem.* **1957**, *61*, 620–622.

0002-7863/81/1503-1922$01.25/0 © 1981 American Chemical Society